Published in final edited form as:
J Pathol. 2014 July ; 233(3): 228–237. doi:10.1002/path.4353.

A genetically engineered ovarian cancer mouse model based on fallopian tube transformation mimics human high-grade serous carcinoma development

Cheryl A. Sherman-Baust[1], **Elisabetta Kuhn**[5], **Blanca L. Valle**[6], **Ie-Ming Shih**[5], **Robert J. Kurman**[5], **Tian-Li Wang**[5], **Tomokazu Amano**[2], **Minoru S.H. Ko**[2], **Ichiro Miyoshi**[3], **Yoshihiko Araki**[4], **Elin Lehrmann**[2], **Yongqing Zhang**[2], **Kevin G. Becker**[2], and **Patrice J. Morin**[1,5,*]

[1] Laboratory of Molecular Biology and Immunology National Institute on Aging, Baltimore MD 21224, USA

[2] Laboratory of Genetics, National Institute on Aging, 251 Bayview Blvd. Baltimore MD 21224, USA

[3] Center for Experimental Animal Science, Nagoya City University Graduate School of Medical Sciences, Nagoya 467-8601, Japan

[4] Institute for Environmental & Gender-Specific Medicine, Juntendo University Graduate School of Medicine, 2-1-1 Tomioka, Urayasu City, Chiba 279-0021, Japan

[5] Department of Pathology, Oncology and Gynecology and Obstetrics Johns Hopkins Medical Institutions, Baltimore, MD 21231, USA

[6] Dept of Otolaryngology Johns Hopkins Medical Institutions, Baltimore, MD 21231, USA

Abstract

Recent evidence suggests that ovarian high-grade serous carcinoma (HGSC) originates from the epithelium of the fallopian tube. However, most mouse models are based on the previous prevailing view that ovarian cancer develops from the transformation of the ovarian surface epithelium. Here, we report the extensive histological and molecular characterization of the mogp-TAg transgenic mouse, which expresses the SV40 large T-antigen (TAg) under the control of the mouse müllerian-specific *Ovgp-1* promoter. Histologic analysis of the fallopian tubes of mogp-TAg mice identified a variety of neoplastic lesions analogous to those described as precursors to ovarian HGSC. We identified areas of normal appearing p53-positive epithelium that are similar to “p53 signatures” in the human fallopian tube. More advanced proliferative lesions with nuclear

* correspondence: Pat J. Morin, Ph.D. Director Scientific Review and Grants Administration American Association for Cancer Research 615 Chestnut St., 17th Floor Philadelphia, PA 191006 Direct: 215.446.7106; Fax: 267.825.9592 pat.morin@aacr.org.

Conflict of interest:
All authors declare no conflicts of interest.

Statement of author contributions:
Cheryl A. Sherman-Baust and Patrice J. Morin conceived and carried out experiments as well as wrote the manuscript. Ichiro Miyoshi and Yoshihiko Araki genetically engineered the mouse model. Tomokazu Amano and Minoru S.H. Ko transferred embryos to establish the model at NIH. Elin Lehrmann, Yongqing Zhang and Kevin G. Becker conducted the microarray experiments and analysis. Blanca L. Valle and Elisabetta Kuhn conducted experiments. Elisabetta Kuhn, Ie-Ming Shih, Robert J. Kurman, and Tian-Li Wang evaluated both the human and mouse IHC/pathology. All authors were involved in reviewing the paper and had final approval of the submitted and published versions.

atypia and epithelial stratification were also identified that were morphologically and immunohistochemically reminiscent of human serous tubal intraepithelial carcinoma (STIC), a potential precursor of ovarian HGSC. Beside these noninvasive precursor lesions, we also identified invasive adenocarcinoma in the ovary of 56% of the mice. Microarray analysis revealed several genes differentially expressed between the fallopian tube of mogp-TAg and wild type (WT) C57BL/6. One of these genes, *Top2a*, which encodes topoisomerase II-alpha, was shown by immunohistochemistry to be concurrently expressed with elevated p53 and specifically elevated in mouse STICs, but not in surrounding tissues. TOP2A protein was also found elevated in human STICs, low-grade, and high-grade serous carcinoma. The mouse model reported here displays a progression from normal tubal epithelium to invasive HGSC in the ovary, and therefore closely simulates the current emerging model of human ovarian HGSC pathogenesis. This mouse therefore has the potential to be a very useful new model for elucidating the mechanisms of serous ovarian tumorigenesis, as well as for developing novel approaches for the prevention, diagnosis, and therapy of this disease.

Keywords

transgenic mouse model; ovarian cancer; fallopian tube; intraepithelial carcinoma; p53; Top2a

Introduction

Epithelial ovarian cancer (EOC) is the most lethal gynecologic malignancy accounting for nearly 15,000 deaths annually in the US, yet the mechanisms of its origin, initiation, and progression remain unclear. In particular, the tissue of origin of EOC has recently become a matter of debate. The ovarian surface epithelium (OSE), a relatively undifferentiated layer of mesothelial cells, has been thought to be the cell of origin, but this theory has several weaknesses [1, 2]. First, precursor lesions of ovarian high-grade serous carcinoma (HGSC), which accounts for the vast majority of EOC, have rarely been identified in the ovary. Second, the various types of EOC have a müllerian origin and phenotype, resembling the epithelia of the endometrium and fallopian tube (FT). In contrast, the ovaries are not müllerian, but rather originate from the genital ridge. Third, in order to account for the similarity of HGSC to FT epithelium, it has been argued that the OSE first undergoes a metaplastic change to tubal-type epithelium before undergoing malignant transformation.

Recently, meticulous reexamination of the FT from women with a predisposition to ovarian cancer has identified malignant lesions in the FT, including early noninvasive precursor lesions of HGSC termed “serous tubal intraepithelial carcinomas” (STICs) [3, 4]. Importantly, STICs have been linked to the development of serous ovarian cancer based on the observation that up to 60% of the patients with sporadic ovarian carcinomas also have STICs in their FTs [5]. In addition, when HGSC and STICs coexist, they exhibit identical p53 mutations [5, 6]. Moreover, morphologically normal-appearing areas of FT epithelium that exhibit p53 staining (termed “p53 signatures”) have been identified in the tubal epithelium and it has been proposed that they represent a precursor to STICs [7]. Taken together, these recent findings suggest a model of ovarian tumorigenesis by which tubal epithelium gives rise to early intraepithelial carcinomas, which can then spread and implant

on the ovary, where they grow and therefore appear to be primary ovarian neoplasms. This theory recapitulates many of the pathologic and morphologic features of human HGSC, including the lack of precursor lesions in the ovary and the histological appearance of HGSC, which resembles FT epithelium.

The majority of genetically engineered mouse models of EOC target the transformation of OSE using various approaches [8-12]. Just recently, Perets et al. reported mouse models with FT transformation that develop high-grade serous tumors that frequently metastasized to the ovary and peritoneum [13]. In light of the evidence for the new paradigm described above, it is crucial to continue to develop mouse models of FT transformation. Here, we report the further characterization of another transgenic mouse, mogp-TAg, which spontaneously develops neoplastic lesions in the FT epithelium and the endometrium [14]. We show that the mouse develops tubal lesions expressing many of the same markers as human STICs and that the transformed FT epithelium often invades the ovary to form tumors similar to human ovarian HGSC. Microarray analysis of the mouse tubal lesions identifies many altered genes and the expression of one of these genes, *Top2A*, is shown to be elevated in mouse and human STICs and may represent a novel early marker in ovarian cancer development.

Materials and Methods

Transgenic mouse

The generation of the mogp-TAg transgenic mouse has been described [14]. Female mice were euthanized at various ages using carbon dioxide inhalation followed by cervical dislocation. The animal protocol was approved by the NIA animal care and use committee.

Tissues

Mouse tissues were either snap frozen for RNA isolation, or fixed in 10% formalin for paraffin embedding. Human archived formalin fixed embedded tissue cases were retrieved from the Johns Hopkins Medical Institutions. 6 STICs, 59 HGSC, 8 low-grade serous carcinomas (LGSC), and 8 normal FTs were included in this study. Tumor tissue was arranged in tissue microarrays. Triplicate 1 mm representative cores were obtained from each tumor block and arrayed on a recipient paraffin block. The collection of specimens was performed in accordance with an approved IRB.

Real-Time RT-PCR

Total RNA was extracted from tissues using Trizol according to the manufacturer's protocol (Invitrogen). Reverse Transcription of 1 μg of total RNA was performed using Taqman Reverse Transcription (Invitrogen). A normal mouse cDNA panel was also used (MNRT 101, OriGene). Primers were designed to amplify the mouse oviductal glycoprotein 1 gene (*Ovgp-1*): ctccacacttgccaaccg (Ovgp1_m2-F) and cataagacgtatggatgatgc (Ovgp1_m2-R). Levels of *Ovgp-1* were analyzed by quantitative real-time PCR using SYBR Green Mix (Roche) normalized to mouse *Gapdh* as previously described [15]. Data was analyzed using the comparative Ct method [16].

Immunohistochemistry (IHC)

IHC of mouse tissues, was accomplished using the Labvision (Fisher) anti-rabbit protocol for the following antibodies: anti-Ki67 at 1:300 (Novus Biologicals); anti-p53 at 1:500 (Santa Cruz); anti-TAg at 1:500 (Santa Cruz); anti-H2AX at 1:500 (Cell Signaling); anti-PAX8 at 1:600 (ProteinTech); anti-Top2A at 1:200 (Epitome) and anti-PBK at 1:25 (Cell Signaling) [17]. For human tissues, IHC was performed as previously described [16]. Briefly, the slides were incubated with antibody against Top2a (Novus Biologicals, cat# NB110-57623) and EnVision™+/HRP Rabbit polymer (Dako, cat# K4003) was then applied. IHC expression for Topoisomerase II Alpha was evaluated as the average percentage of nuclear positive tumor cells on 3 tissue cores of the tissue array.

Illumina microarray analysis

Total RNA was extracted from the FTs of three wild-type C57BL/6 mice and three mogp-TAg mice using Trizol (Invitrogen). Biotinylated cRNA was prepared from 500 ng of RNA using the Illumina RNA Amplification Kit (Ambion). The cDNA was hybridized to a MouseRef-8 Expression BeadChip (Illumina). Microarray data analysis was performed as previously described [18]. Expression changes for individual genes were considered significant if they met 4 criteria: z-ratio above 1.5; false detection rate <0.30; p-value of the pairwise t-test<0.05; and mean background-corrected signal intensity z-score in each comparison group is not negative [19]. Principal component analysis was conducted based on the above values using JMP software (SAS) to generate a 3D scatterplot with percent variance. These data have been deposited in NCBI's Gene Expression Omnibus and is accessible through GEO Series accession number GSE52011 (http://www.ncbi.nlm.nih.gov/geo/query/acc.cgi?acc=GSE52011). Ingenuity Pathway Analysis (IPA) was also conducted, looking at both canonical pathways and biological functions (Ingenuity® Systems).

Statistical analysis

Comparisons of IHC outcomes were performed using the two-tailed unpaired t-test. p-values of 0.05 or less were considered statistically significant. Statistical analysis was carried out using GraphPad Prism software (GraphPad Software).

Results

TAg expressing transgenic mouse

Gene expression profiling data showed that *OVGP1* is highly expressed in the epithelium of the human FT, but is found at much lower levels in other tissues (data not shown). In order to assess the value of the *Ovgp1* promoter in a mouse model of FT transformation, we evaluated the expression pattern of *Ovgp1* in 34 mouse tissues by real-time RT-PCR. We found that *Ovgp1* is expressed 45-fold higher in the FT compared to any other female tissue (Supp. Fig. 1). The testis expressed the highest levels of *Ovgp1* in males, albeit at a lower level than in FTs. We therefore hypothesized that the *Ovgp1* promoter may be used to specifically induce tumorigenesis in the FT through expression of the TAg. We decided to further characterize the previously reported mogp-TAg mouse, which expresses TAg from

the mouse *Ovgp1* promoter [14]. Starting at approximately 6 weeks of age, tumors of the female genital tract were found in mogp-TAg females. As the females aged, we observed an increase in size of both the uterus and the FTs.

Histopathologic and immunohistochemical analysis of the FTs

Analysis of the FTs of mice 7-12 weeks of age, led to the identification of lesions that were overtly malignant, characterized by epithelial stratification and marked nuclear atypia, including mitotic bodies, enlarged nuclei, and irregular chromatin, resembling what has been described as STICs in human FTs [20-22] (Fig. 1). A human STIC is shown in inset for comparison. These lesions, which we refer to as mSTICs, were positive for p53 and expressed the TAg. Similar to what is observed in human STICs, mSTICs were also highly proliferative as ascertained by Mib-1 (Ki-67) staining (Fig. 1).

Because of reports describing “p53 signatures” in human HGSC, [7, 22, 23] we searched for similar lesions in this model. We identified areas in the FT mucosa of mice between 6-9 weeks of age that exhibited intense p53 staining, but did not show morphological signs of a carcinoma (Fig. 2). Again, TAg staining was restricted to a small area that corresponded to the p53 staining. The mouse p53 signature shown in Fig. 2 exhibited high proliferation, as most of the cells present in the lesion were Mib-1 positive. p53 signatures and mSTICs were observed in all the mice examined except older mice (13 weeks) where the presence of advanced epithelial lesions had completely destroyed the tissue. The stroma of mogp-TAg mice exhibited staining of both TAg and Mib-1 (Figs 1 and 2), while the WT mice did not (data not shown).

Invasive adenocarcinoma in the ovary

In addition to tubal lesions, adenocarcinomas were detected in the ovaries of 56% of mogp-TAg mice examined between the ages of 8-10 weeks (Fig. 3). No adenocarcinomas were found in younger mice. The invasive carcinomas were positive for TAg and p53, and exhibited a high proliferation index, as determined by Mib-1 staining. Interestingly, these carcinomas were positive for PAX8, a müllerian/FT marker, while the surrounding ovarian tissues, including the OSE, were negative. The invasive cancers also stained positively for γ–H2AX, a marker of DNA damage that has been shown to be positive in human STICs and in serous cancers [24]. It is interesting to note that all mice with HGSCs also had p53 signatures and STICs in their FTs.

Gene expression profiling of neoplastic FTs

In order to better understand the molecular mechanism of tumorigenesis in the FT, we compared gene expression profiles of FT from mogp-TAg mice with WT age-matched FTs. Microarray analysis identified a large number of genes whose expression was altered in mogp-TAg FT. Principal Component Analysis (PCA) revealed a distinct gene expression pattern between the FT from mogp-TAg mice and WT mice (Fig. 4). We chose to focus our attention on genes that were elevated in the diseased FT, as we hypothesized that these genes may represent useful biomarkers for mSTICs and mouse p53 signatures, and possibly provide insight into the mechanisms of HGSC initiation. Table 1 lists the top 20 most highly up-regulated genes in mogp-TAg FT compared to WT FT. Six of these genes have

previously been reported to be regulated by p53, which highlights this prominent signaling mechanism in the neoplastic FT tissues. IPA analysis revealed alterations in many Canonical pathways (Supp. Fig. 2, Supp. Table 1). As expected, p53 Signaling was affected (Supp. Fig. 3, Supp. Table 2). The most significantly modified pathways included Cell Cycle Control of Chromosomal Replication (Supp. Fig. 4, Supp. Table 3) and the Role of BRCA1 in DNA Damage Response (Supp. Fig. 5, Supp. Table 4). Also, expression patterns seen in biological outcomes (Ingenuity defined functions) (Supp. Fig. 6) such as cancer, and reproductive system diseases were identified.

Topoisomerase II alpha is elevated in mouse high-grade serous lesions

Tumorigenesis is initiated by p53 inactivation in this model and is a very early event in human serous carcinoma development as well. Therefore, we were particularly interested in the p53-regulated genes identified as altered in mogp-TAg FT, as they may represent genuine targets of p53 in serous carcinoma development. In particular, we focused on PDZ binding kinase (*Pbk*) and Topoisomerase II alpha (*Top2a*), which have previously been implicated in human cancer [25, 26]. We performed IHC for PDZ binding kinase and Topoisomerase II alpha on mouse sections from WT and mogp-TAg FT. *Pbk* staining did not show reproducible patterns (data not shown), and was not investigated further. *Top2a* exhibited strong staining in mSTICs and in the invasive portion of the tumor (Fig. 5). In particular, there was a striking correlation between the expression of *Top2a* and the expression of p53 in these samples, suggesting strongly that *Top2a* is regulated by p53 in this HGSC model. The signaling involved is highlighted in the IPA pathway analysis finding, G2/M DNA Damage Checkpoint Regulation (Supp. Fig. 7, Supp. Table 5).

Topoisomerase II alpha is elevated in human high-grade serous lesions

In order to determine whether *TOP2A* was also expressed in human serous carcinoma, we stained human STICs and serous carcinoma for Topoisomerase II alpha expression (Fig. 6). Human STICs and HGSCs exhibited strong diffuse staining of Topoisomerase II alpha, while LGSC cells exhibited sparse staining at best and normal FT cells were negative. The transition in staining between normal FT and STIC was particularly striking, with a complete absence of staining in normal FT transitioning to strong staining in the STIC (Fig. 6). Quantitative analysis of 8 normal human FT epithelium (NFT), 8 LGSCs , 59 HGSCs, and 6 STICs demonstrated statistically significant differences in Topoisomerase II alpha expression between NFT and LGCS (P=0.0001), HGSC (P=0.0039), and STICs (P=0.0013) (Fig 6F). In addition, statistically significant differences were found between LGSC and both STICs (P=0.0054) and HGSC (P=0.011). There was no significant difference in the between STIC and HGSC (P=0.40).

Discussion

Technological advances have allowed the development of genetically engineered mouse models that recapitulate genotypic and phenotypic features of human cancers [27]. In ovarian cancer, multiple genetically engineered mouse models have been reported but, because of the prevailing view that HGSCs develop from the ovarian surface epithelium, most are based on the transformation of mouse OSE.

Recently, a series of morphologic, immunohistochemical and molecular studies have suggested that epithelial cells in the distal tube (fimbria) give rise to ovarian (pelvic) HGSC [28, 29]. According to this theory, secretory cells in the tube can clonally proliferate, and through a series of intermediate steps, give rise to intraepithelial serous carcinoma, which can either invade the tube before spreading to the ovary, or can shed cells that implant directly on the ovary and surrounding pelvic structures. Here, we present a transgenic model which expresses the TAg from the mouse *Ovgp1* promoter, a müllerian-specific promoter highly active in the FT. The use of the TAg in the induction of FT carcinogenesis is appropriate, considering that p53 inactivation appears to be one of the earliest events in this cancer [29]. While the OVGP promoter is ideal for targeting the TAg to the fallopian tube, its activity is dependent on estrogen. Subsequently, the expression of TAg corresponds with sexual maturity of the mice and with the onset of the serous lesions in our model. The ability to control TAg expression could actually be quite useful. In principle, this could be done by performing an ovariectomy on young mice to inhibit estrogen production and then add estrogen artificially to induce tumorigenesis.

The TAg used in our mouse model binds p53 and is thought to completely inactivate the protein, leading to a p53-null phenotype (although the p53 protein accumulates due to a lack of degradation of the complex). The majority of p53 mutations observed in ovarian cancer are point mutations that also lead to protein inactivation and accumulation. However, based on several lines of evidence, mutant p53 protein may have residual activity or even acquire novel activities that promote transformation. Therefore, our model may not be completely representative of the p53 phenotype in the majority of ovarian cancers. However, it is important to realize that up to 30% of ovarian cancer have a null p53 phenotype indicating that complete p53 inactivation is indeed a mechanism that is observed with this disease [30]. It has been suggested that, while the gain-of-function mutations of p53 may not be essential for tumor development, they may be important in some other aspects of tumorigenesis such as drug resistance.

It is important to note that the large T antigen inactivates both p53 and Rb. While the Rb gene itself is not frequently mutated in ovarian cancer, the Rb pathway is likely altered in a large proportion of ovarian cancers. Indeed, mutations in INK4, RB, or CDK4 were observed in almost fifty percent of ovarian samples [31, 32]. In addition, specifically analyzing p16 expression and alteration, numerous studies have reported changes in up to 65% of ovarian cancers. Inactivation of pRB in addition to p53 in our model may therefore be consistent with human ovarian tumorigenesis.

Examination of the FT of the mogp-TAg mice revealed the presence of several neoplastic lesions, including a mouse equivalent to the human STIC, mSTIC. In addition, we also found morphologically normal lesions that stained for p53, analogous to the p53 signatures in humans. Similar to what is observed in human p53 signatures, we believe that the accumulated p53 in the mouse is non-functional, as it is bound to the large TAg. Interestingly, the TAg expression showed patterns identical to the p53 signatures, which indicates that the pattern of p53 stabilization and inactivation is due to the variations in the expression or binding of the TAg. The mouse p53 signatures were proliferative as determined by Ki-67 staining. Proliferative p53 signatures have been identified in human

FTs and are thought to be an intermediate step between p53 signatures with low Ki-67 and STICs, which typically have a high proliferation index [29]. While the p53 signature patterns cannot be explained at this time, they nonetheless make this mouse model quite interesting as it appears to be very similar to the of early ovarian cancer development. Another particularly provocative finding was the observation of adenocarcinomas within the ovary. Nine of the 16 mice we examined contained a carcinoma implant in one or both ovaries. All were positive for PAX 8 expression, a müllerian marker found overexpressed in human ovarian HGSC [33], and for γ-H2AX, a marker of DNA damage also found expressed in serous cancer [34]. Overall, these findings are consistent with the theory suggesting that human ovarian HGSC originates in the FT. While it is possible that the carcinoma observed within the mouse ovaries originated in the OSE, we believe it is unlikely for several reasons: 1) we did not observe TAg expression in any other areas of the ovary, including the OSE, 2) the carcinomas in the ovary were positive for PAX8, a known marker of müllerian tissues that is negative in OSE [35], and 3) despite extensive serial sectioning, we did not find continuity between the ovarian carcinoma and the OSE.

The majority of previous ovarian cancer mouse models relied on OSE transformation and yielded either undifferentiated or poorly differentiated carcinomas [9, 11, 36], endometrioid carcinomas [36, 37], cystic adenocarcinomas [10] and leiomyosarcomas [37-40] but not high grade adenocarcinomas as seen in humans and the mogp-TAg mouse. While these mice have taught us a great deal about OSE transformation, the findings are not surprising considering that the OSE is mesothelial in nature and not müllerian as the majority of EOC appear. The mogp-TAg mouse is not the only model that targets FT epithelium. Kim et al. [41] reported a conditional knock out of Dicer and Pten in tubal epithelium that was shown to produce carcinomas and metastasis. However, the primary tumors were reported to arise from the FT stroma not the epithelium, which is not believed to be the case in human HGSC. More recently, a study demonstrated that deletion of Trp53, Pten, and Brca1/2 in the FT secretory cells leads to HGSC that frequently metastasized to the ovary [13]. This finding is consistent with our model, which shows that FT transformation can lead to HGSC and serous carcinoma to the ovary. A feature of the mogp-TAg mouse is that it exhibits easily identifiable precursor lesions (p53 signatures and STICs). The presence of these precursors in the FT is particularly important because it can potentially shed light on the early events of high-grade serous tumorigenesis.

The *Ovgp1* promoter used for TAg expression was specific as we did not observe cancer outside the genital tract in females. However, the FT stroma was found to express TAg and Mib-1. While we did not observe neoplastic lesions in the FT stroma, the ovarian stromal compartment has been suggested to affect tumor progression, and therefore the behavior of the epithelial FT cells may be affected by the abnormal TAg expressing stroma. This model may therefore be useful in the study of the effects of the environment in ovarian cancer initiation and development. In addition, examination of the uterus of older mice also revealed neoplastic lesions. We observed non-invasive malignant lesions, reminiscent of endometrial intraepithelial carcinoma (EIC) (data not shown), the precursor of uterine serous carcinoma (USC) in humans. Finally, we did observe non-invasive sarcomas in the uterus of older mice, which is consistent with the observation that this stroma also expresses the TAg.

While the sarcoma is certainly an unwanted byproduct of *Ovgp1*-mediated TAg expression, we do not believe that it affects the epithelial phenotype seen in the model.

The gene expression patterns were clearly different between normal and diseased tissue (Fig. 4), which allowed the identification of multiple genes and pathways abnormally regulated in the mogp FTE. IPA revealed that cell cycle control and DNA damage response pathways were altered in the FT of mogp-TAg mice. This is consistent with our strategy for inducing tumorigenesis, inactivation of p53, but also with the known mechanisms of ovarian cancer initiation and development. Moreover, the p53 pathway itself was prominently deregulated with multiple downstream genes abnormally expressed. *Top2a*, a gene previously shown to be regulated by p53 [42] and implicated in breast cancer development [25, 43], was shown to be elevated in mSTICs, the early HGSC lesions identified in our mouse model. TP53 and Top2a were concurrently expressed in the lesions, a finding consistent with previous observations made in advanced ovarian cancer samples [44]. Most interestingly, we also found TOP2A elevated in human STICs and ovarian cancer, not only validating our mouse model as relevant to human ovarian cancer, but also identifying a new biomarker for early serous lesions. TOP2A is a target for anthracyclines, such as doxorubicin, a drug used in platinum-refractory ovarian cancer and its expression has been associated with poor survival and platinum resistance in ovarian cancer [45]. It has also been reported that TOP2A is elevated in tumor-adjacent stroma cells, but decreased in tumor cells following chemotherapy [46], suggesting that TOP2A may also have an important role in the stroma. In any case, our model may represent a useful tool to study the roles of TOP2A in ovarian cancer development and drug resistance.

In summary, we report a new ovarian cancer model based on transformation of FT epithelium. The model exhibits features strongly reminiscent of STICs in humans and, importantly, also displays serous adenocarcinoma implants in the ovary. The model may therefore represent a useful tool for the study of ovarian cancer progression. In addition, since the model recapitulates the earliest events in serous ovarian cancer development, it may be useful in the identification of novel strategies for prevention as well as for treatment of this disease.

Supplementary Material

Refer to Web version on PubMed Central for supplementary material.

Acknowledgments

We thank the members of our laboratory for useful comments on the manuscript. This research was supported in part by the Intramural Research Program of the NIH, National Institute on Aging and by US Department of Defense grant, W81XWH-11-2-0230/OC100517.

List of Abbreviations

HGSC	high-grade serous carcinoma
FT	fallopian tube

OSE	ovarian surface epithelium
TAg	SV40 large T-antigen
STIC	serous tubal intraepithelial carcinoma
EOC	Epithelial ovarian cancer
H&E	hematoxylin and eosin
TMA	tissue microarrays
EIC	endometrial intraepithelial carcinoma
USC	uterine serous carcinoma
FTE	fallopian tube epithelium
NFT	normal human FT epithelium
LGSC	Low Grade Serous Carcinoma

References

1. Dubeau L. The cell of origin of ovarian epithelial tumors and the ovarian surface epithelium dogma: does the emperor have no clothes? Gynecol Oncol. 1999; 72:437–442. [PubMed: 10053122]
2. Kurman RJ, Shih Ie M. Pathogenesis of ovarian cancer: lessons from morphology and molecular biology and their clinical implications. Int J Gynecol Pathol. 2008; 27:151–160. [PubMed: 18317228]
3. Medeiros F, Muto MG, Lee Y, et al. The tubal fimbria is a preferred site for early adenocarcinoma in women with familial ovarian cancer syndrome. Am J Surg Pathol. 2006; 30:230–236. [PubMed: 16434898]
4. Finch A, Shaw P, Rosen B, et al. Clinical and pathologic findings of prophylactic salpingo-oophorectomies in 159 BRCA1 and BRCA2 carriers. Gynecologic oncology. 2006; 100:58–64. [PubMed: 16137750]
5. Kindelberger DW, Lee Y, Miron A, et al. Intraepithelial carcinoma of the fimbria and pelvic serous carcinoma: Evidence for a causal relationship. Am J Surg Pathol. 2007; 31:161–169. [PubMed: 17255760]
6. Kuhn E, Kurman RJ, Vang R, et al. TP53mutations in serous tubal intraepithelial carcinoma and concurrent pelvic high-grade serous carcinoma- evidence supporting the clonal relationship of the two lesions. The Journal of pathology. 2011
7. Lee Y, Miron A, Drapkin R, et al. A candidate precursor to serous carcinoma that originates in the distal fallopian tube. The Journal of pathology. 2007; 211:26–35. [PubMed: 17117391]
8. Orsulic S, Li Y, Soslow RA, et al. Induction of ovarian cancer by defined multiple genetic changes in a mouse model system. Cancer Cell. 2002; 1:53–62. [PubMed: 12086888]
9. Connolly DC, Bao R, Nikitin AY, et al. Female mice chimeric for expression of the simian virus 40 TAg under control of the MISIIR promoter develop epithelial ovarian cancer. Cancer Research. 2003; 63:1389–1397. [PubMed: 12649204]
10. Flesken-Nikitin A, Choi KC, Eng JP, et al. Induction of carcinogenesis by concurrent inactivation of p53 and Rb1 in the mouse ovarian surface epithelium. Cancer Res. 2003; 63:3459–3463. [PubMed: 12839925]
11. Laviolette LA, Garson K, Macdonald EA, et al. 17beta-estradiol accelerates tumor onset and decreases survival in a transgenic mouse model of ovarian cancer. Endocrinology. 2010; 151:929–938. [PubMed: 20056833]

12. Mullany LK, Fan HY, Liu Z, et al. Molecular and functional characteristics of ovarian surface epithelial cells transformed by KrasG12D and loss of Pten in a mouse model in vivo. Oncogene. 2011; 30:3522–3536. [PubMed: 21423204]
13. Perets R, Wyant GA, Muto KW, et al. Transformation of the fallopian tube secretory epithelium leads to high-grade serous ovarian cancer in Brca;Tp53;Pten models. Cancer Cell. 2013; 24:751–765. [PubMed: 24332043]
14. Miyoshi I, Takahashi K, Kon Y, et al. Mouse transgenic for murine oviduct-specific glycoprotein promoter-driven simian virus 40 large T-antigen: tumor formation and its hormonal regulation. Mol Reprod Dev. 2002; 63:168–176. [PubMed: 12203826]
15. Rangel LBA, Agarwal R, D'Souza T, et al. Tight Junction Proteins Claudin-3 and Claudin-4 Are Frequently Overexpressed in Ovarian Cancer but Not in Ovarian Cystadenomas. Clin Cancer Res. 2003; 9:2567–2575. [PubMed: 12855632]
16. Livak KJ, Schmittgen TD. Analysis of relative gene expression data using real-time quantitative PCR and the 2(-Delta Delta C(T)) Method. Methods. 2001; 25:402–408. [PubMed: 11846609]
17. Ramos-Vara JA. Technical aspects of immunohistochemistry. Veterinary pathology. 2005; 42:405–426. [PubMed: 16006601]
18. Gleichmann M, Zhang Y, Wood WH 3rd, et al. Molecular changes in brain aging and Alzheimer's disease are mirrored in experimentally silenced cortical neuron networks. Neurobiol Aging. 2012; 33:205, e201–205, e218. [PubMed: 20947216]
19. Cheadle C, Vawter MP, Freed WJ, et al. Analysis of microarray data using Z score transformation. J Mol Diagn. 2003; 5:73–81. [PubMed: 12707371]
20. Sehdev AS, Kurman RJ, Kuhn E, et al. Serous tubal intraepithelial carcinoma upregulates markers associated with high-grade serous carcinomas including Rsf-1 (HBXAP), cyclin E and fatty acid synthase. Mod Pathol. 2010; 23:844–855. [PubMed: 20228782]
21. Carlson JW, Miron A, Jarboe EA, et al. Serous tubal intraepithelial carcinoma: its potential role in primary peritoneal serous carcinoma and serous cancer prevention. Journal of clinical oncology : official journal of the American Society of Clinical Oncology. 2008; 26:4160–4165. [PubMed: 18757330]
22. Jarboe E, Folkins A, Nucci MR, et al. Serous carcinogenesis in the fallopian tube: a descriptive classification. Int J Gynecol Pathol. 2008; 27:1–9. [PubMed: 18156967]
23. Shaw PA, Rouzbahman M, Pizer ES, et al. Candidate serous cancer precursors in fallopian tube epithelium of BRCA1/2 mutation carriers. Mod Pathol. 2009; 22:1133–1138. [PubMed: 19543244]
24. Folkins AK, Jarboe EA, Saleemuddin A, et al. A candidate precursor to pelvic serous cancer (p53 signature) and its prevalence in ovaries and fallopian tubes from women with BRCA mutations. Gynecol Oncol. 2008; 109:168–173. [PubMed: 18342932]
25. Brase JC, Schmidt M, Fischbach T, et al. ERBB2 and TOP2A in breast cancer: a comprehensive analysis of gene amplification, RNA levels, and protein expression and their influence on prognosis and prediction. Clin Cancer Res. 2010; 16:2391–2401. [PubMed: 20371687]
26. Park JH, Lin ML, Nishidate T, et al. PDZ-binding kinase/T-LAK cell-originated protein kinase, a putative cancer/testis antigen with an oncogenic activity in breast cancer. Cancer Res. 2006; 66:9186–9195. [PubMed: 16982762]
27. Frese KK, Tuveson DA. Maximizing mouse cancer models. Nature reviews Cancer. 2007; 7:645–658.
28. Kurman RJ, Shih Ie M. The origin and pathogenesis of epithelial ovarian cancer: a proposed unifying theory. Am J Surg Pathol. 2010; 34:433–443. [PubMed: 20154587]
29. Mehrad M, Ning G, Chen EY, et al. A pathologist's road map to benign, precancerous, and malignant intraepithelial proliferations in the fallopian tube. Adv Anat Pathol. 2010; 17:293–302. [PubMed: 20733351]
30. Brachova P, Thiel KW, Leslie KK. The consequence of oncomorphic TP53 mutations in ovarian cancer. Int J Mol Sci. 2013; 14:19257–19275. [PubMed: 24065105]
31. Hashiguchi Y, Tsuda H, Yamamoto K, et al. Combined analysis of p53 and RB pathways in epithelial ovarian cancer. Hum Pathol. 2001; 32:988–996. [PubMed: 11567230]

32. Kusume T, Tsuda H, Kawabata M, et al. The p16-cyclin D1/CDK4-pRb pathway and clinical outcome in epithelial ovarian cancer. Clin Cancer Res. 1999; 5:4152–4157. [PubMed: 10632354]
33. Laury AR, Perets R, Piao H, et al. A comprehensive analysis of PAX8 expression in human epithelial tumors. Am J Surg Pathol. 2011; 35:816–826. [PubMed: 21552115]
34. Jarboe EA, Pizer ES, Miron A, et al. Evidence for a latent precursor (p53 signature) that may precede serous endometrial intraepithelial carcinoma. Modern Pathology. 2009; 22:345–350. [PubMed: 19151662]
35. Bowen NJ, Logani S, Dickerson EB, et al. Emerging roles for PAX8 in ovarian cancer and endosalpingeal development. Gynecologic oncology. 2007; 104:331–337. [PubMed: 17064757]
36. Dinulescu DM, Ince TA, Quade BJ, et al. Role of K-ras and Pten in the development of mouse models of endometriosis and endometrioid ovarian cancer. Nat Med. 2005; 11:63–70. [PubMed: 15619626]
37. Wu R, Hendrix-Lucas N, Kuick R, et al. Mouse model of human ovarian endometrioid adenocarcinoma based on somatic defects in the Wnt/beta-catenin and PI3K/Pten signaling pathways. Cancer Cell. 2007; 11:321–333. [PubMed: 17418409]
38. Clark-Knowles KV, Garson K, Jonkers J, et al. Conditional inactivation of Brca1 in the mouse ovarian surface epithelium results in an increase in preneoplastic changes. Exp Cell Res. 2007; 313:133–145. [PubMed: 17070800]
39. Quinn BA, Brake T, Hua X, et al. Induction of ovarian leiomyosarcomas in mice by conditional inactivation of Brca1 and p53. PLoS One. 2009; 4:e8404. [PubMed: 20046879]
40. Szabova L, Yin C, Bupp S, et al. Perturbation of Rb, p53, and Brca1 or Brca2 cooperate in inducing metastatic serous epithelial ovarian cancer. Cancer Res. 2012; 72:4141–4153. [PubMed: 22617326]
41. Kim J, Coffey DM, Creighton CJ, et al. High-grade serous ovarian cancer arises from fallopian tube in a mouse model. Proceedings of the National Academy of Sciences of the United States of America. 2012
42. Kwon Y, Shin BS, Chung IK. The p53 tumor suppressor stimulates the catalytic activity of human topoisomerase IIalpha by enhancing the rate of ATP hydrolysis. J Biol Chem. 2000; 275:18503–18510. [PubMed: 10764786]
43. Di Leo A, Gancberg D, Larsimont D, et al. HER-2 amplification and topoisomerase IIalpha gene aberrations as predictive markers in node-positive breast cancer patients randomly treated either with an anthracycline-based therapy or with cyclophosphamide, methotrexate, and 5-fluorouracil. Clin Cancer Res. 2002; 8:1107–1116. [PubMed: 12006526]
44. Bar JK, Grelewski P, Noga L, et al. The association between the p53/topoisomerase I and p53/topoisomerase IIalpha immunophenotypes and the progression of ovarian carcinomas. Adv Clin Exp Med. 2012; 21:35–42. [PubMed: 23214297]
45. Kucukgoz Gulec U, Gumurdulu D, Guzel AB, et al. Prognostic importance of survivin, Ki-67, and topoisomerase IIalpha in ovarian carcinoma. Arch Gynecol Obstet. 2013
46. Chekerov R, Klaman I, Zafrakas M, et al. Altered expression pattern of topoisomerase IIalpha in ovarian tumor epithelial and stromal cells after platinum-based chemotherapy. Neoplasia. 2006; 8:38–45. [PubMed: 16533424]

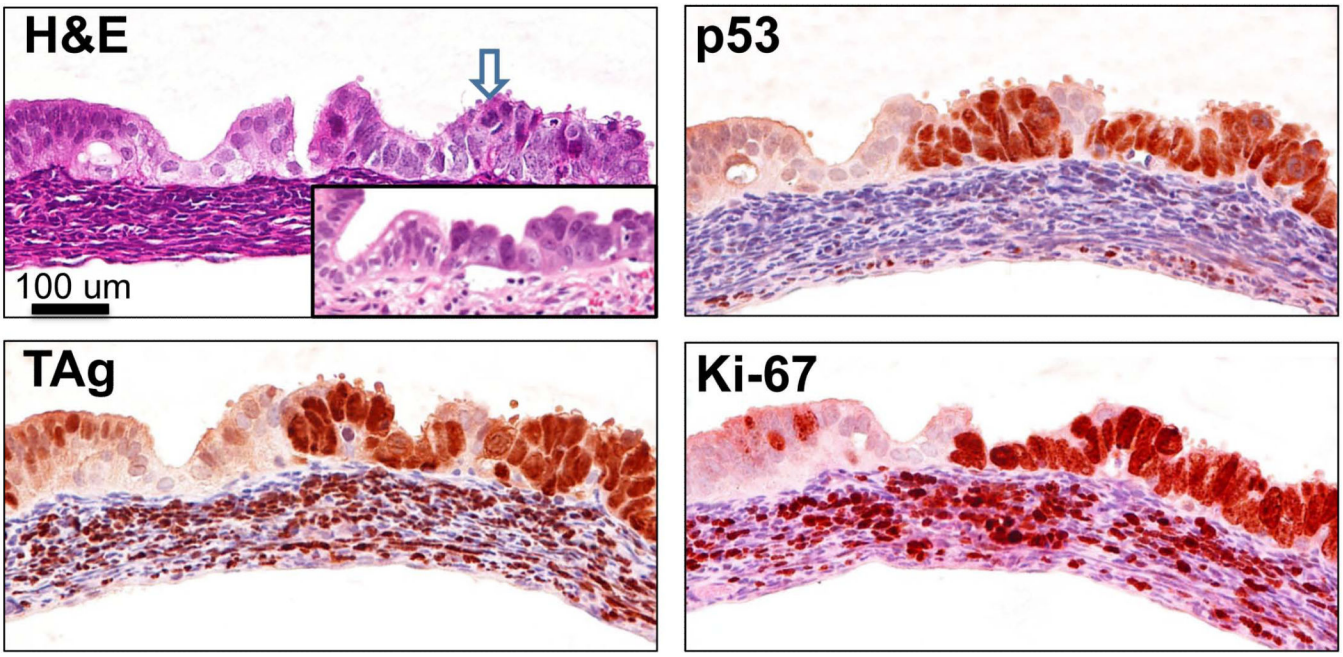

Figure 1. mogp-TAg FT contains lesions (mSTICs) similar to human STICs

H&E staining of a representative 7-8 week old mogp-TAg FT. The blue arrow points to the presence of a lesion, mSTIC, with abnormal chromatin, epithelial stratification, apoptotic bodies and nuclear enlargement, all characteristics of human STICs (human STIC shown in inset for comparison). Adjacent serial sections with immunohistochemical staining against TAg, p53, and Ki-67. All three markers exhibit intense and diffuse positive staining in the mSTIC area of the FT epithelium. Ki-67 and TAg are positive in the stromal area as well.

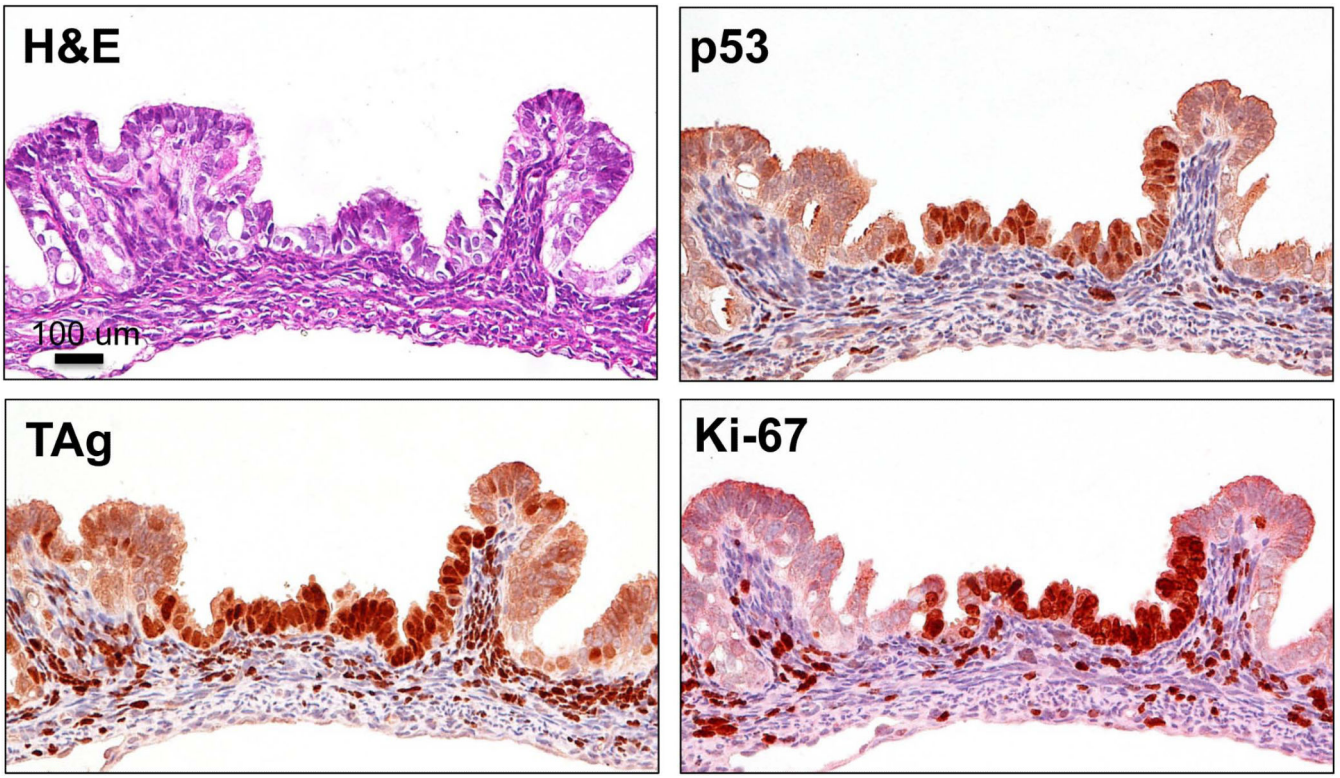

Figure 2. Mouse p53 signature

H&E staining of a typical 6 week old female mogp-TAg mouse shows an area of the epithelium, which appears morphologically normal. Immunohistochemical staining with p53 shows strongly positive and diffuse staining of a portion of the normal FT epithelium: the mouse p53 signature. The area also exhibits staining for TAg in the p53 signature. Ki-67 staining in the mouse p53 signature indicates that the lesion is proliferative.

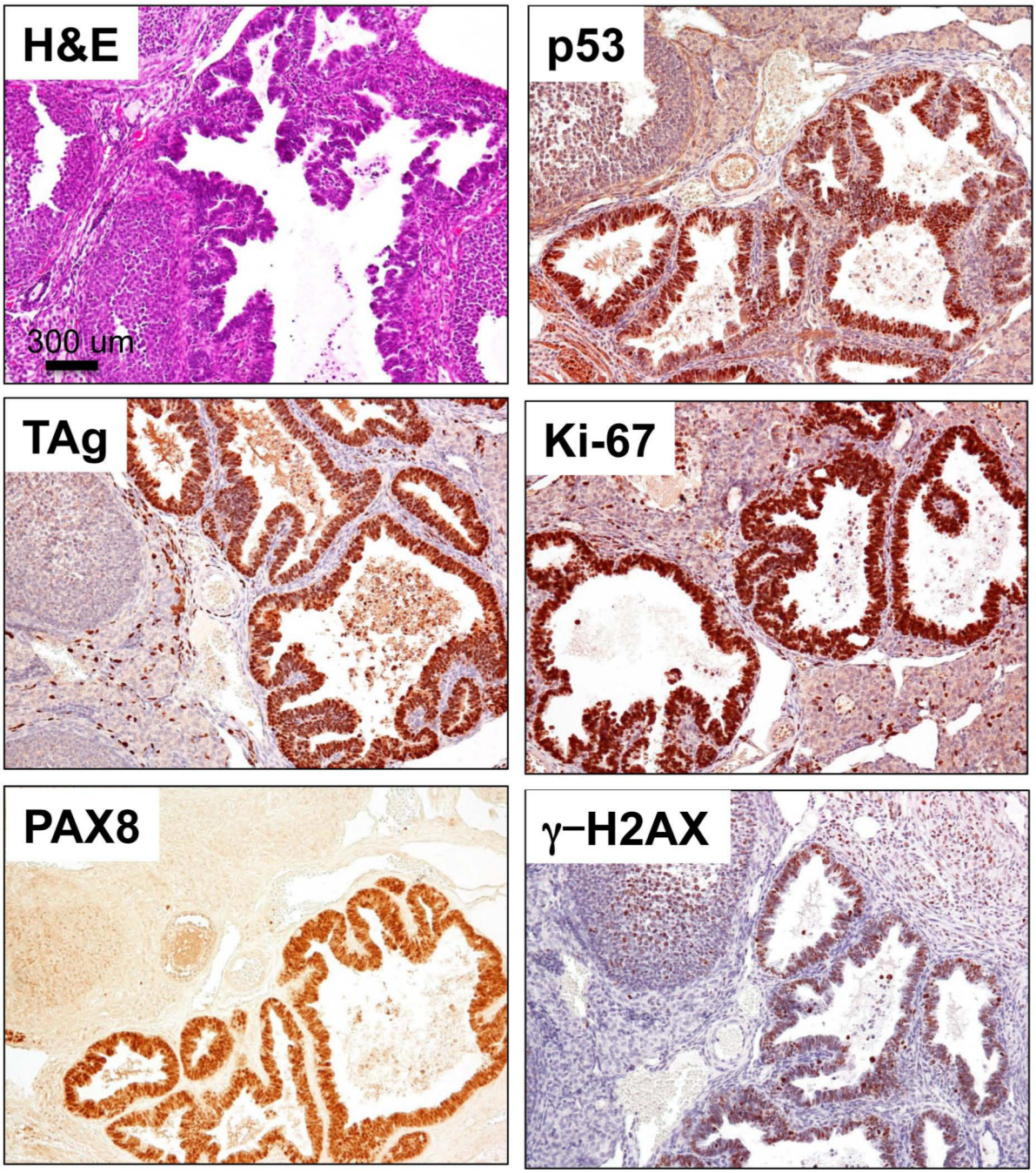

Figure 3. Invasive carcinoma of the ovary

H&E of the ovary a 10 week old mouse shows the pathological features of the invasive serous carcinoma that include papillary structures and condensed chromatin. TAg IHC is strongly positive in the stratified epithelium of the invasive carcinoma. The carcinogenic area also demonstrates strong staining for p53, Ki-67, the müllerian marker PAX8 and γ-H2AX. 56% of the mice examined have similar carcinomas in their ovaries.

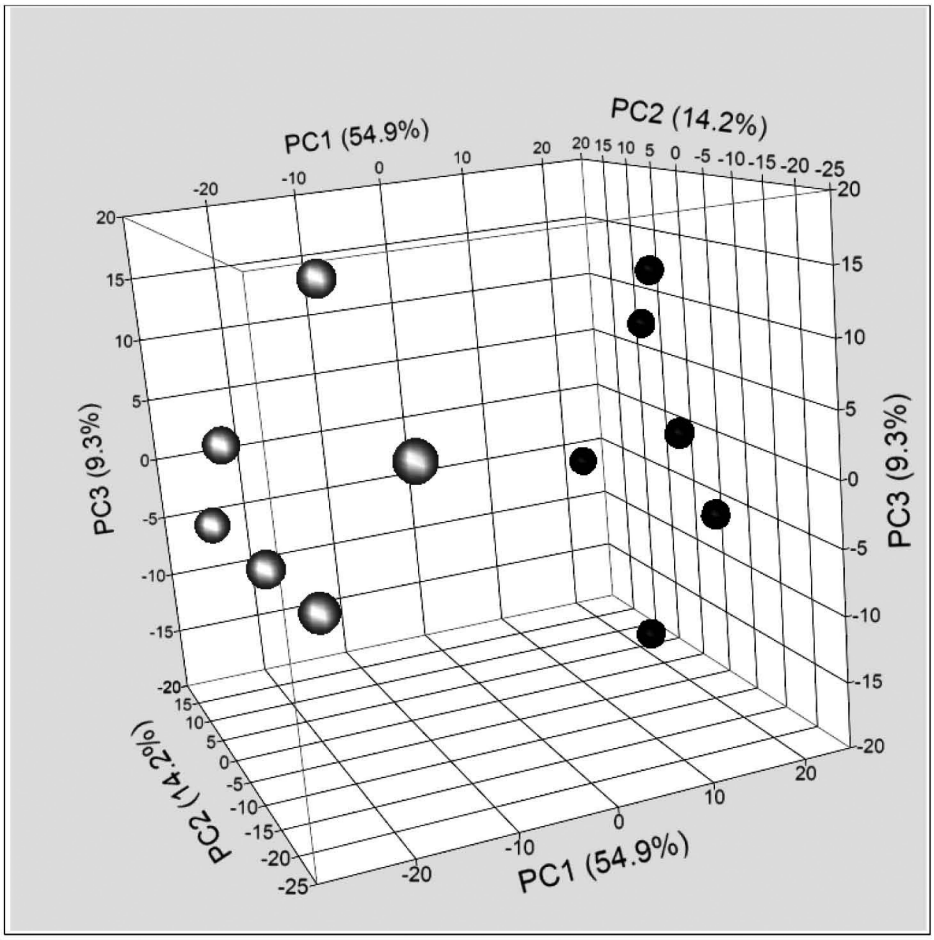

Figure 4. Principal component analysis of gene expression in mogp-TAg and WT mice

FT from mogp-TAg mice (represented by white/grey filled circles) showed a distinct pattern of gene expression compared to FT form WT mice (black filled circles) as depicted both by the PCI values and the visual appearance of the 3D scatterplot.

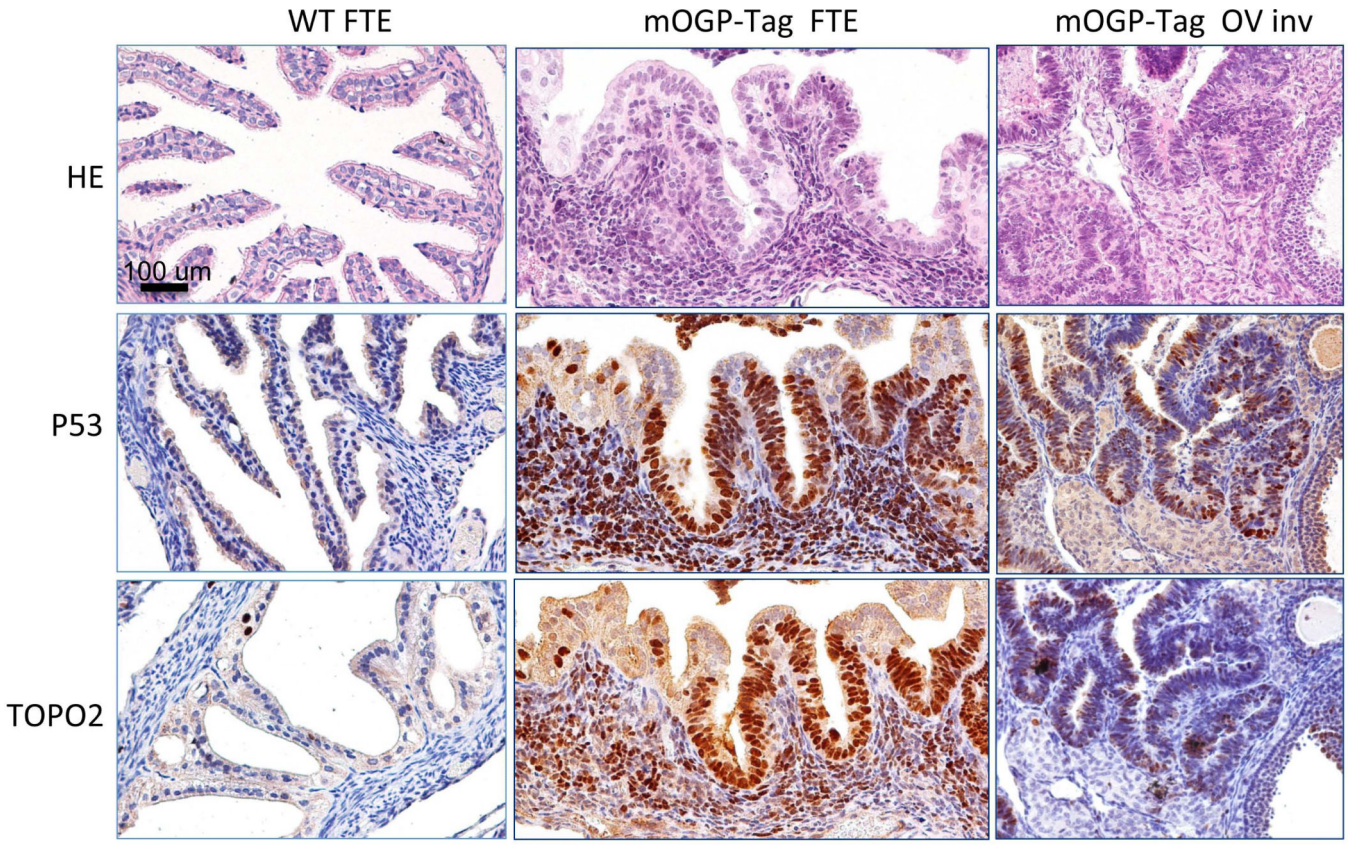

Figure 5. TP53 (tumor protein p53) and Top2a (Topoisomerase II alpha) are concurrently expressed in mogp-TAg mouse lesions

WT C57BL/6 FT epithelium, mogp-TAg FT epithelium (FTE) and metastatic mogp-TAg ovary were stained with H&E (top row), P53 antibody (Middle row), or Top2a antibody (bottom row). These serial sections of representative organs show concurrent IHC staining for both p53 and Top2a.

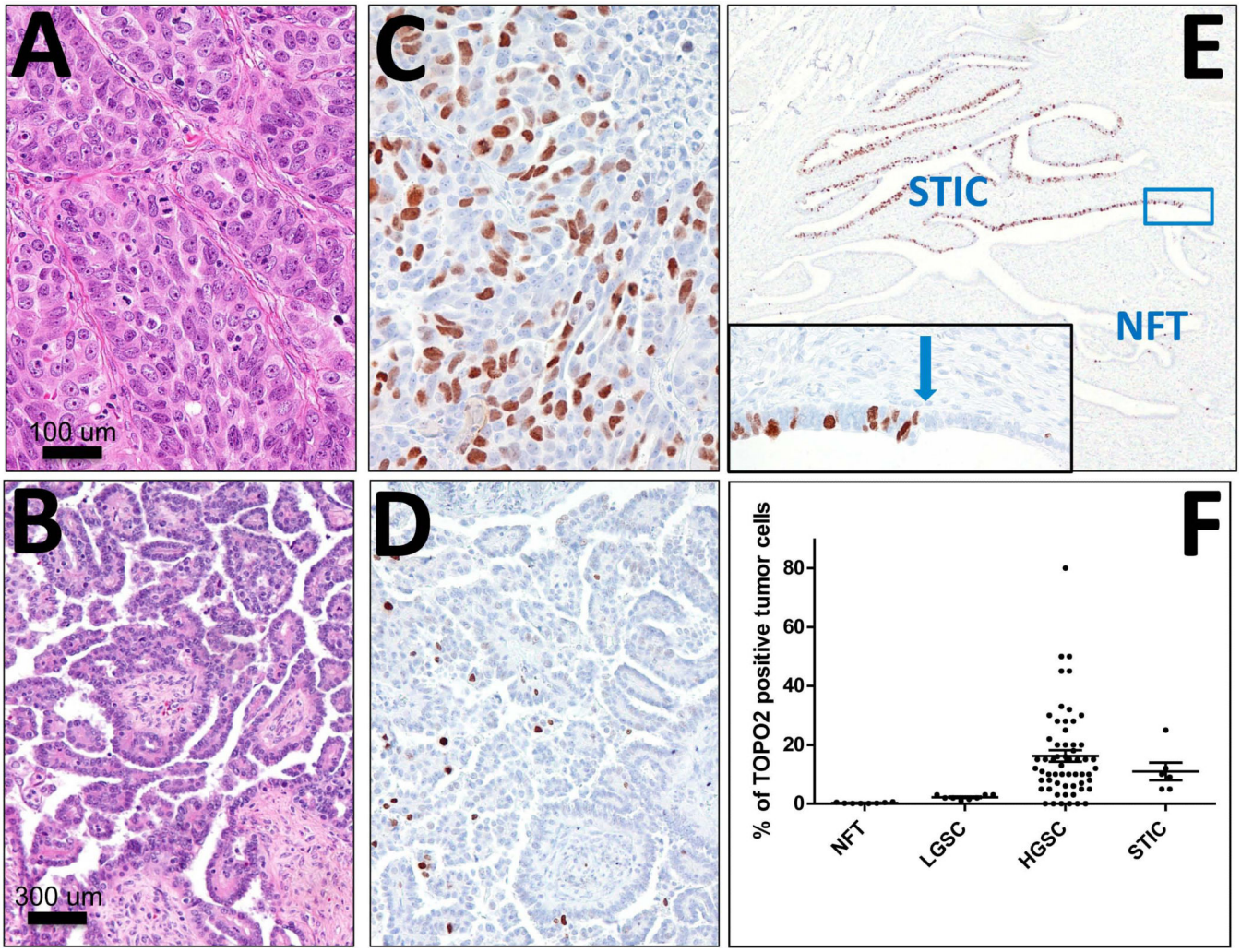

Figure 6. Human Topoisomerase II alpha IHC

High-grade serous carcinoma (A, C) and Human FT STICs (STICs) display strong diffuse Topoisomerase II alpha staining. Low-grade serous carcinoma (B, D) exhibits sparse staining and normal human FT epithelium (NFT) is negative. Blue arrow indicates the transition site from normal epithelium to a STIC. A, C: H&E staining; B, D, E: TOP2A immunostaining. F. Expression levels of Top2a were evaluated in normal human FT epithelium samples (NFT), Low Grade Serous Carcinoma samples (LGSC), High Grade Serous Carcinoma samples (HGSC), and Serous Tubal Intraepithelial Carcinoma samples (STIC). The most significant differences are found between NFT and carcinomas: LGSC, HGCD and STICs. There is also a significant difference between LGSC and both STICs and HGSC. There is no significant difference between STIC and HGSC.

Table 1

Top 20 up regulated genes in mogp-TAg mouse FT relative to wild-type FT

Gene Name	Gene Symbol	Z ratio	Fold Change
proline-rich acidic protein 1	Prap1	13.38	38.26
aldo-keto reductase family 1, member B7	Akr1b7	10.37	17.53
protein regulator of cytokinesis 1	Prc1	10.53	14.48
histone cluster 1, H2ad	Hist1h2ad	9.69	11.50
histone cluster 1, H2ah	Hist1h2ah	9.51	11.29
PDZ binding kinase	Pbk	9.31	11.03
topoisomerase (DNA) II alpha	Top2a	8.98	10.37
histone cluster 1, H2ak	Hist1h2ak	9.57	9.57
minichromosome maintenance deficient 5	Mcm5	8.76	9.41
centromere protein A	Cenpa	8.42	8.75
cyclin B1	Ccnb1	8.18	8.59
cadherin 16	Cdh16	8.05	8.53
histone cluster 1, H2af	Hist1h2af	8.55	8.41
nucleolar and spindle associated protein 1	Nusap1	8.21	8.41
cyclin-dependent kinase 1	Cdc2a	7.88	8.26
histone cluster 1, H2ag	Hist1h2ag	8.12	8.21
kinesin family member 23	Kif23	7.96	8.06
histone cluster 1, H2ao	Hist1h2ag	8.26	8.04
cell division cycle associated 3	Cdca3	8.07	7.96
baculoviral IAP repeat-containing 5	Birc5	7.87	7.78

Note: Shaded cells highlight those genes known to be regulated by TP53